Applied Physics Letters ACCEPTED MANUSCRIPT

This is the author's peer reviewed, accepted manuscript. However, the online version of record will be different from this version once it has been copyedited and typeset.

PLEASE CITE THIS ARTICLE AS DOI: 10.1063/1.5131001

Observation of anomalous Ettingshausen effect and large transverse thermoelectric conductivity in permanent magnets

Asuka Miura[1,2], Hossein Sepehri-Amin[1], Keisuke Masuda[1], Hiroki Tsuchiura[3,4], Yoshio Miura[1,5], Ryo Iguchi[1], Yuya Sakuraba[1,6], Junichiro Shiomi[2], Kazuhiro Hono[1], and Ken-ichi Uchida[1,2,4,7,a)]

AFFILIATIONS

[1] National Institute for Materials Science, Tsukuba 305-0047, Japan
[2] Department of Mechanical Engineering, The University of Tokyo, Tokyo 113-8656, Japan
[3] Department of Applied Physics, Tohoku University, Sendai 980-8579, Japan
[4] Center for Spintronics Research Network, Tohoku University, Sendai 980-8577, Japan
[5] Center for Spintronics Research Network, Osaka University, Osaka 560-8531, Japan
[6] PRESTO, Japan Science and Technology Agency, Saitama 332-0012, Japan
[7] Institute for Materials Research, Tohoku University, Sendai 980-8577, Japan
[a)]Author to whom correspondence should be addressed: UCHIDA.Kenichi@nims.go.jp

ABSTRACT

This study focuses on the potential of permanent magnets as thermoelectric converters. It is found that a $SmCo_5$-type magnet exhibits the large anomalous Ettingshausen effect (AEE) at room temperature and that its charge-to-heat current conversion coefficient is more than one order of magnitude greater than that of typical ferromagnetic metals. The large AEE is an exclusive feature of the $SmCo_5$-type magnet among various permanent magnets in practical use, which is independent of the conventional performance of magnets based on static magnetic properties. The experimental results show that the large AEE originates from the intrinsic transverse thermoelectric conductivity of $SmCo_5$. This finding makes a connection between permanent magnets and thermal energy engineering, providing the basis for creating "thermoelectric permanent magnets."

The Ettingshausen effect is a transverse thermoelectric conversion phenomenon in a conductor, which refers to the generation of a heat current in the direction perpendicular to a charge current and an external magnetic field.[1] With the hope of developing highly efficient

26 May 2024 05:25:59

Applied Physics Letters ACCEPTED MANUSCRIPT
This is the author's peer reviewed, accepted manuscript. However, the online version of record will be different from this version once it has been copyedited and typeset.
PLEASE CITE THIS ARTICLE AS DOI: 10.1063/1.5131001
AIP Publishing
26 May 2024 05:25:59

thermoelectric cooling systems, the Ettingshausen effect in Bi and Bi-based compounds was investigated many decades ago.[2,3] However, using an Ettingshausen cooler is problematic as its operation requires huge external magnetic fields. One of the avenues to overcome this problem is the use of the anomalous Ettingshausen effect (AEE)[4-14] in magnetic materials, which generates a heat current in the direction of the cross product of a charge current and spontaneous magnetization:

$$\mathbf{j}_{q,AEE} = \Pi_{AEE}\left(\mathbf{j}_c \times \mathbf{m}\right), \quad (1)$$

where $\mathbf{j}_{q,AEE}$, $\mathbf{j}_c$, $\mathbf{m}$, and Π_{AEE} denote the heat current density driven by AEE, charge current density, unit vector of the magnetization, and anomalous Ettingshausen coefficient,[11] respectively. As AEE works as a temperature modulator even in the absence of external magnetic fields and requires no complex junction structures, it may develop thermal management technologies for electronic and spintronic devices. The advantages of the AEE-based thermoelectric conversion also include the facts that the direction of heat currents can be controlled simply by changing the magnetization direction and that the thermoelectric output of the AEE device follows a simple scaling law; the cooling and heat power can be enhanced by lengthening the dimension of the device along the heat current. These advantages originate from the symmetry of Eq. (1), which were impossible with conventional thermoelectric conversion based on the Peltier effect. However, AEE has been observed only in several ferromagnetic metals.[9-14] To realize highly efficient AEE-driven thermoelectric conversion, detailed physics and material investigations using various classes of materials are necessary. Finding and developing magnetic materials with large Π_{AEE} are also important for the realization of energy-harvesting and heat-sensing applications based on the anomalous Nernst effect (ANE),[15-23] which is the Onsager reciprocal of AEE.

In this study, we report the observation of AEE in permanent magnets at room temperature. Among the various permanent magnets in practical use, we found that the $SmCo_5$-type magnets exhibit prominently large Π_{AEE} values, which are more than one order of magnitude larger than typical values for ferromagnetic metals, such as Ni. The figure of merit for AEE in $SmCo_5$-type magnets is comparable to the record value obtained for the ANE in a full-Heusler ferromagnet.[20] Although the thermoelectric performance needs to be improved for practical applications, our finding represents a significant step toward the realization of the AEE-based temperature modulators for the following reasons. First, in permanent magnets with large remanent magnetization and coercivity, the AEE-induced temperature change is generated in the absence of external magnetic fields in a wide temperature range (note that, in the case of

Applied Physics Letters ACCEPTED MANUSCRIPT
This is the author's peer reviewed, accepted manuscript. However, the online version of record will be different from this version once it has been copyedited and typeset.
PLEASE CITE THIS ARTICLE AS DOI: 10.1063/1.5131001
AIP Publishing

SmCo$_5$-type magnets, the remanent magnetization typically remains stable up to ~300 °C). This is in sharp contrast to the conventional Ettingshausen effect, which shows good performance only at high magnetic fields and low temperatures.[2,3] Second, permanent magnets are mass-produced and widely used; adding thermoelectric conversion functionalities to permanent magnets may contribute to the development of various energy-saving technologies. Third, our results stimulate physics and material research on AEE because transverse thermoelectric phenomena in permanent magnets have not been investigated yet.

The observation of AEE in permanent magnets is realized by means of the lock-in thermography (LIT) method.[9-14,24-27] This method makes it possible to demonstrate the symmetry of AEE and quantitatively estimate its thermoelectric performance without applying magnetic fields. We measured the thermal images of the surface of permanent magnets while applying a square-wave-modulated alternating charge current $\mathbf{J}_c$ with the amplitude J_c, frequency f, and zero offset to the magnets in the x direction and extracted the first harmonic response of the detected images, which are transformed into lock-in amplitude A and phase ϕ images through Fourier analysis. Based on this procedure, the pure contribution of thermoelectric effects ($\propto J_c$) can be detected independently from the Joule-heating background ($\propto J_c^2$) [Fig. 1(f)].[9-14,26,27] To confirm the symmetry of AEE, we performed the LIT measurements for permanent magnets in both the in-plane and perpendicularly magnetized configurations at room temperature, where $\mathbf{m}$ is directed along the $+z$ and $+y$ directions, respectively [Fig. 1(a),(b)]. Following Eq. (1), the heat current driven by AEE in the in-plane (perpendicularly) magnetized configuration is generated in the y (z) direction. The experimental details are shown in Section S1 in supplementary material.

Figure 1(c),(d) shows the A and ϕ images of the SmCo$_5$-type magnet slab at f=2.0 Hz and J_c=0.4 A. The slab is almost fully magnetized in the absence of magnetic fields because its remanent magnetization ($\mu_0 M_r$=0.96 T with μ_0 being the vacuum permeability) is comparable to the saturation magnetization ($\mu_0 M_s$=1.01 T) (Table S1 in supplementary material). In the in-plane magnetized configuration, clear current-induced temperature modulation was observed on the entire surface of the SmCo$_5$ slab [Fig. 1(c)]. As the input charge current and output temperature change oscillate with the same phase, the temperature of the sample surface increases when $\mathbf{J}_c$ flows in the $-x$ direction. Importantly, the same SmCo$_5$ slab in the perpendicularly magnetized configuration shows the temperature increase and decrease in the left and right halves, respectively [Fig. 1(d)]; the magnitude of the temperature change varies almost linearly in the z direction and its sign is reversed at the center of the sample [see the A

26 May 2024 05:25:59

Applied Physics Letters ACCEPTED MANUSCRIPT
This is the author's peer reviewed, accepted manuscript. However, the online version of record will be different from this version once it has been copyedited and typeset.
PLEASE CITE THIS ARTICLE AS DOI: 10.1063/1.5131001
AIP Publishing

and ϕ profiles in Fig. 1(d) and note that the ϕ difference between the left and right halves is ~180°]. This temperature distribution is in good agreement with the symmetry of AEE [see Eq. (1) and compare Fig. 1(c),(d) with 1(a),(b)]. We confirmed that the magnitude of the temperature modulation of the $SmCo_5$ slab is proportional to J_c and consistent with the feature of AEE[9-14] [Fig. 1(e)]. As demonstrated here, LIT enables the pure detection of AEE in permanent magnets without applying external magnetic fields.

To quantitatively estimate the anomalous Ettingshausen coefficient, the behavior of the AEE-induced temperature modulation in a steady state must be known. In general, LIT images measured at low lock-in frequency show temperature distributions in nearly steady states, while those at high lock-in frequency show temperature distributions in transient states, where temperature broadening due to thermal diffusion is suppressed.[10,24] Thus, we measured the f dependence of the LIT images of the $SmCo_5$ slab that gives information on the AEE-induced temperature modulation in the steady state. Figure 2 shows that the magnitude of the AEE signals in the $SmCo_5$ slab monotonically increases with decreasing f. The f dependence of the AEE signals is well reproduced by solving the one-dimensional heat diffusion equation in the frequency domain (Section S2 in supplementary material). Based on the results in Fig. 2, the amplitude of the AEE-induced temperature modulation per unit charge current density for our $SmCo_5$ slab in the steady state, i.e., at f=0 Hz, is estimated to be $A/j_c=6.3\times10^{-8}$ $KA^{-1}m^2$, where j_c is the amplitude of the square-wave-modulated charge current density. Surprisingly, this value is much greater than that of typical ferromagnetic metals; we obtained $A/j_c=0.1\times10^{-8}$ $KA^{-1}m^2$ for a Ni slab with the same thickness and width as the $SmCo_5$ slab (see Fig. 2 and note that the magnitude of A/j_c is proportional to the length along the AEE-induced heat current[13]). By substituting the steady-state AEE signals into Eq. (1), the anomalous Ettingshausen coefficient of the $SmCo_5$-type magnet is estimated to be $\Pi_{AEE}=9.4\times10^{-4}$ V, which is more than one order of magnitude larger than that of Ni (0.7×10^{-4} V). The corresponding anomalous Nernst coefficient of the $SmCo_5$-type magnet at the temperature T=300 K is given by $S_{ANE}=\Pi_{AEE}/T=3.1\times10^{-6}$ VK^{-1} via the Onsager reciprocal relation.[11]

Here, we show the relation between AEE in permanent magnets and their static magnetic properties. To clarify the dependence of AEE on the saturation magnetization, we performed the LIT measurements under the same condition using various $SmCo_5$-type magnets with different $\mu_0 M_s$ values ranging from 0.66 T to 1.01 T, where M_s is reduced by partially substituting Sm with Gd and comparable to M_r for all the magnets as shown in Table S1 in supplementary material (note that the $SmCo_5$ slab used for the experiments in Figs. 1 and 2

26 May 2024 05:25:59

Applied Physics Letters ACCEPTED MANUSCRIPT
This is the author's peer reviewed, accepted manuscript. However, the online version of record will be different from this version once it has been copyedited and typeset.
PLEASE CITE THIS ARTICLE AS DOI: 10.1063/1.5131001
AIP Publishing

contains negligibly small amounts of Gd and the electronic structure of $SmCo_5$ near the Fermi energy is barely affected by the substitution of Sm with Gd).[28-31] Interestingly, despite the crucial difference in the magnetization and composition, we obtained almost the same Π_{AEE} values for the $SmCo_5$-type magnets [Fig. 3(a)]. We also confirmed that the AEE signals are independent of the difference in the microstructure of the magnets, which affects the coercivity and resulting maximum energy product (Section S3 in supplementary material). These results indicate that the large AEE originates from an intrinsic property of $SmCo_5$. Furthermore, we found that, among the three types of rare-earth permanent magnets in practical use, i.e., the $SmCo_5$-, Sm_2Co_{17}-, and $Nd_2Fe_{14}B$-type magnets, only the $SmCo_5$-type magnets exhibit the large AEE, although the Sm_2Co_{17}- and $Nd_2Fe_{14}B$-type magnets have larger magnetization [Fig. 3(a)]. This behavior clearly deviates from the scaling between the magnetization and transverse thermoelectric effects.[18]

Significantly, the performance of the $SmCo_5$-type magnets as the AEE/ANE-based thermoelectric converters reaches a record high. The figure of merit for AEE/ANE is defined as[11,32]

$$Z_{AEE}T = \frac{\Pi_{AEE}^2 \sigma_{xx}}{\kappa}\frac{1}{T} \quad \left(= \frac{S_{ANE}^2 \sigma_{xx}}{\kappa} T\right). \tag{2}$$

By measuring the longitudinal electric conductivity σ_{xx} and the thermal conductivity κ, we estimated the $Z_{AEE}T$ values of the magnets. As shown in Fig. 3(b), we found no correlation between $Z_{AEE}T$ and $\mu_0 M_s$ in each type of magnet. The maximum $Z_{AEE}T$ value of the $SmCo_5$-type magnet is 4.5×10^{-4} at T=300 K, which is two orders (one order) of magnitude greater than that of Ni (Sm_2Co_{17}- and $Nd_2Fe_{14}B$-type magnets) and comparable to the value of full-Heusler Co_2MnGa that exhibits the remarkably large ANE.[20-22]

Now, we are in a position to discuss the origin of the large AEE in the $SmCo_5$-type magnets. Based on the Onsager reciprocal relation between AEE and ANE, the anomalous Ettingshausen coefficient can be divided into the following two terms:[20,23]

$$\Pi_{AEE} = \left(\rho_{xx}\alpha_{xy} + \rho_{xy}\alpha_{xx}\right)T \equiv \Pi_I + \Pi_{II}, \tag{3}$$

where $\rho_{xx}=1/\sigma_{xx}$ ($\rho_{xy}=-\sigma_{xy}/\sigma_{xx}^2$) denotes the diagonal (off-diagonal) component of the electric resistivity tensor, α_{xx} (α_{xy}) the diagonal (off-diagonal) component of the thermoelectric conductivity tensor, $\Pi_I=\rho_{xx}\alpha_{xy}T$, and $\Pi_{II}=\rho_{xy}\alpha_{xx}T$. In Eq. (3), we assume a fully magnetized ferromagnet and disregard the magnetic-field-dependent contributions in the electric and thermoelectric transport coefficients. The contribution of Π_I is often regarded as an intrinsic part of AEE as it originates from the transverse thermoelectric conductivity α_{xy}, which is

26 May 2024 05:25:59

Applied Physics Letters ACCEPTED MANUSCRIPT
This is the author's peer reviewed, accepted manuscript. However, the online version of record will be different from this version once it has been copyedited and typeset.
PLEASE CITE THIS ARTICLE AS DOI: 10.1063/1.5131001
AIP Publishing

determined by the energy derivative of the anomalous Hall conductivity σ_{xy} (Section S4 in supplementary material).[20,23] In contrast, the contribution of Π_{II} is attributed to the concerted action of the Seebeck effect and anomalous Hall effect (AHE), and can be rewritten as $\Pi_{II}=S_{xx}T\tan\theta_{AHE}$, where $S_{xx}=\rho_{xx}\alpha_{xx}$ and $\theta_{AHE}=\rho_{xy}/\rho_{xx}$ are the Seebeck coefficient and anomalous Hall angle, respectively. To estimate Π_{II}, we measured the Seebeck effect and AHE in the $SmCo_5$-, Sm_2Co_{17}-, and $Nd_2Fe_{14}B$-type magnets at room temperature. Figure 4(a) shows the Hall resistivity ρ_{Hall} of the magnets as a function of the magnetic field μ_0H. The magnets exhibit clear hysteresis loops in the μ_0H-ρ_{Hall} curves; the AHE contribution can be extracted by extrapolating the ρ_{Hall} data in the high-field region to the zero field. The obtained θ_{AHE} values are negative for all the magnets and the magnitude of θ_{AHE} of the $SmCo_5$-type magnet is smaller than that of the Sm_2Co_{17}- and $Nd_2Fe_{14}B$-type magnets [Fig. 4(b)]. The inset to Fig. 4(b) shows that σ_{xy} of the magnets is almost independent of σ_{xx}, suggesting that AHE in these materials is in the intrinsic regime in the scaling relation.[15] By combining the AHE data with the Seebeck coefficient in Fig. 4(c), we obtained the Π_{II} values for the $SmCo_5$-, Sm_2Co_{17}-, and $Nd_2Fe_{14}B$-type magnets at T=300 K. As shown in Fig. 4(d), Π_{II} is positive for the magnets, the sign of which is the same as (opposite to) that of Π_{AEE} for the $SmCo_5$- and Sm_2Co_{17}-type magnets ($Nd_2Fe_{14}B$-type magnet). The magnitude of Π_{II} for the $SmCo_5$-type magnet is much smaller than that of Π_{AEE}, indicating that AEE is dominated by the Π_I term owing to the large transverse thermoelectric conductivity [Fig. 4(d)]. The estimated α_{xy} value of the $SmCo_5$-type magnet (4.6 $K^{-1}Am^{-1}$) is much larger than those of the Sm_2Co_{17}-type magnet (0.6 $K^{-1}Am^{-1}$) and the $Nd_2Fe_{14}B$-type magnet (–0.9 $K^{-1}Am^{-1}$) and, surprisingly, even larger than that of Co_2MnGa at room temperature (2.4-3.0 $K^{-1}Am^{-1}$).[20] This remarkably large α_{xy} can be the intrinsic property of $SmCo_5$, which is supported by our first-principles calculations; the α_{xy} value calculated from the electronic structures of $SmCo_5$ is comparable to the experimental value (Section S4 in supplementary material). However, more detailed theoretical investigations, such as the calculations of the Berry curvature and its contribution to AEE, are necessary to clarify the microscopic mechanism of the transverse thermoelectric response in the $SmCo_5$-type magnets.

Although the $SmCo_5$-type magnet exhibits a record-high α_{xy} value, its thermoelectric performance is still insufficient for practical applications, and further investigations are required to explore and develop magnets with larger $Z_{AEE}T$. Judging from the previous discussions on the thermoelectric conversion efficiency for ANE, $Z_{AEE}T$>0.1 is necessary for practical applications.[32,33] Based on the results for $SmCo_5$, $Z_{AEE}T$>0.1 can be obtained, for

26 May 2024 05:25:59

Applied Physics Letters ACCEPTED MANUSCRIPT
This is the author's peer reviewed, accepted manuscript. However, the online version of record will be different from this version once it has been copyedited and typeset.
PLEASE CITE THIS ARTICLE AS DOI: 10.1063/1.5131001

example, by realizing 10 times enhancement of Π_{AEE} and 50% reduction of κ simultaneously [see Eq. (2)]. A clue for the improvement of Π_{AEE} is included in our first-principles calculations; carrier doping of $SmCo_5$ may modulate the transverse transport coefficients and increase the resulting Π_{AEE} (Section S4 in supplementary material). Furthermore, as AEE originates from the spin-orbit interaction acting on spin-polarized electron transport, the substitution of Co with heavy elements possessing strong spin-orbit interaction, such as Pt and Pd, can be another strategy for enhancing the intrinsic contribution of Π_{AEE}. The κ reduction is achievable by nanostructuring[34] and grain boundary engineering,[35] although the $SmCo_5$-type magnet used in this study has no grain boundary phases (Section S3 in supplementary material). The grain boundary engineering may also modulate extrinsic spin-orbit interaction and spin-transport properties in the magnets,[35] which have a potential to improve the transverse thermoelectric response.

In conclusion, we investigated the transverse thermoelectric conversion properties in the well-known rare-earth magnets and observed the large AEE in the $SmCo_5$-type magnets. This result is the first step towards the creation of "thermoelectric permanent magnets"; such multi-functional materials will invigorate fundamental studies in spin caloritronics and thermoelectrics, and develop thermal energy management and harvesting technologies for electronic and spintronic devices. Importantly, in contrast to conventional soft magnetic materials, thermoelectric permanent magnets can modulate temperature or generate electricity in the absence of external magnetic fields. Although the selection of conventional magnets is determined by the maximum energy product and maximum usable temperature, this multi-functionality and versatility may change the selection criteria for permanent magnets and lead to unconventional applications. We thus anticipate that the proof-of-concept demonstration reported here will provide a basis for exploring and developing magnets with larger $Z_{AEE}T$.

See supplementary material for more details on the experimental procedure, calculations of the f dependence of the AEE signals, microstructure analysis of the $SmCo_5$-type magnets, and first-principles calculations of the transverse transport properties.

The authors thank Y. Hirayama, X. Tang, T. Seki, M. Matsumoto, H. Adachi, M. Shimizu, and H. O. Jeschke for valuable discussions. This work was supported by CREST "Creation of Innovative Core Technologies for Nano-enabled Thermal Management" (JPMJCR17I1), PRESTO "Phase Interfaces for Highly Efficient Energy Utilization" (JPMJPR12C1), and

26 May 2024 05:25:59

Applied Physics Letters ACCEPTED MANUSCRIPT
This is the author's peer reviewed, accepted manuscript. However, the online version of record will be different from this version once it has been copyedited and typeset.
PLEASE CITE THIS ARTICLE AS DOI: 10.1063/1.5131001
AIP Publishing
26 May 2024 05:25:59

PRESTO "Scientific Innovation for Energy Harvesting Technology" (JPMJPR17R5) from JST, Japan; Grant-in-Aid for Scientific Research (S) (JP18H05246) and Grant-in-Aid for Early-Career Scientists (JP18K14116) from JSPS KAKENHI, Japan; and the NEC Corporation. A.M. is supported by JSPS through Research Fellowship for Young Scientists (JP18J02115).

REFERENCES

[1] A. V. Ettingshausen and W. Nernst, Ann. Phys. **265**, 343 (1886).
[2] K. F. Cuff, R. B. Horst, J. L. Weaver, S. R. Hawkins, C. F. Kooi, and G. M. Enslow, Appl. Phys. Lett. **2**, 145 (1963).
[3] T. C. Harman, J. M. Honig, S. Fischler, A. E. Paladino, and M. J. Button, Appl. Phys. Lett. **4**, 77 (1964).
[4] P. W. Bridgman, Phys. Rev. **24**, 644 (1924).
[5] E. H. Hall, Phys. Rev. **26**, 820 (1925).
[6] E. Butler Jr. and E. Pugh, Phys. Rev. **57**, 916 (1940).
[7] G. E. W. Bauer, E. Saitoh, and B. J. van Wees, Nat. Mater. **11**, 391 (2012).
[8] S. R. Boona, R. C. Myers, and J. P. Heremans, Energy Environ. Sci. **7**, 885 (2014).
[9] T. Seki, R. Iguchi, K. Takanashi, and K. Uchida, Appl. Phys. Lett. **112**, 152403 (2018).
[10] K. Uchida, S. Daimon, R. Iguchi, and E. Saitoh, Nature **558**, 95 (2018).
[11] T. Seki, R. Iguchi, K. Takanashi, and K. Uchida, J. Phys. D: Appl. Phys. **51**, 254001 (2018).
[12] R. Iguchi, A. Yagmur, Y. C. Lau, S. Daimon, E. Saitoh, M. Hayashi, and K. Uchida, Phys. Rev. B **98**, 014402 (2018).
[13] R. Das, R. Iguchi, and K. Uchida, Phys. Rev. Appl. **11**, 034022 (2019).
[14] S. Ota, K. Uchida, R. Iguchi, P. V. Thach, H. Awano, and D. Chiba, Sci. Rep. **9**, 13197 (2019).
[15] T. Miyasato, N. Abe, T. Fujii, A. Asamitsu, S. Onoda, Y. Onose, N. Nagaosa, and Y. Tokura, Phys. Rev. Lett. **99**, 086602 (2007).
[16] Y. Sakuraba, K. Hasegawa, M. Mizuguchi, T. Kubota, S. Mizukami, T. Miyazaki, and K. Takanashi, Appl. Phys. Express **6**, 033003 (2013).
[17] K. Uchida, T. Kikkawa, T. Seki, T. Oyake, J. Shiomi, Z. Qiu, K. Takanashi, and E. Saitoh, Phys. Rev. B **92**, 094414 (2015).
[18] M. Ikhlas, T. Tomita, T. Koretsune, M. Suzuki, D. Nishio-Hamane, R. Arita, Y. Otani, and S. Nakatsuji, Nat. Phys. **13**, 1085 (2017).

Applied Physics Letters ACCEPTED MANUSCRIPT
This is the author's peer reviewed, accepted manuscript. However, the online version of record will be different from this version once it has been copyedited and typeset.
PLEASE CITE THIS ARTICLE AS DOI: 10.1063/1.5131001
AIP Publishing

[19] Z. Yang, E. A. Codecido, J. Marquez, Y. Zheng, J. P. Heremans, and R. C. Myers, AIP Adv. **7**, 095017 (2017).

[20] A. Sakai, Y. P. Mizuta, A. A. Nugroho, R. Sihombing, T. Koretsune, M. Suzuki, N. Takemori, R. Ishii, D. Nishio-Hamane, R. Arita, P. Goswami, and S. Nakatsuji, Nat. Phys. **14**, 1119 (2018).

[21] H. Reichlova, R. Schlitz, S. Beckert, P. Swekis, A. Markou, Y. C. Chen, D. Kriegner, S. Fabretti, G. H. Park, A. Niemann, S. Sudheendra, A. Thomas, K. Nielsch, C. Felser, and S. T. B. Goennenwein, Appl. Phys. Lett. **113**, 212405 (2018).

[22] S. N. Guin, K. Manna, J. Noky, S. J. Watzman, C. G. Fu, N. Kumar, W. Schnelle, C. Shekhar, Y. Sun, J. Gooth, and C. Felser, NPG Asia Mater. **11**, 16 (2019).

[23] Y. Sakuraba, K. Hyodo, A. Sakuma, and S. Mitani, arXiv:1807.02209.

[24] O. Breitenstein, W. Warta, and M. Langenkamp, *Lock-in thermography: Basics and Use for Evaluating Electronic Devices and Materials Introduction*. (Springer, Berlin/Heidelberg, Germany, 2010).

[25] O. Wid, J. Bauer, A. Muller, O. Breitenstein, S. S. P. Parkin, and G. Schmidt, Sci. Rep. **6**, 28233 (2016).

[26] S. Daimon, R. Iguchi, T. Hioki, E. Saitoh, and K. Uchida, Nat. Commun. **7**, 13754 (2016).

[27] K. Uchida, R. Iguchi, S. Daimon, R. Ramos, A. Anadón, I. Lucas, P. A. Algarabel, L. Morellón, M. H. Aguirre, M. R. Ibarra, and E. Saitoh, Phys. Rev. B **95**, 184437 (2017).

[28] Z. Tie-Song, J. Han-Min, G. Guang-Hua, H. Xiu-Feng, and C. Hong, Phys. Rev. B **43**, 8593 (1991).

[29] S. Liu and G. E. Kuhl, IEEE Trans. Magn. **35**, 3271 (1999).

[30] W. Y. Zhang, A. R. Yan, H. W. Zhang, S. Y. Zhang, and B. G. Shen, J. Phys. D: Appl. Phys. **34**, 1065 (2001).

[31] S. K. Malik, F. J. Arlinghaus, and W. E. Wallace, Phys. Rev. B **16**, 1242 (1977).

[32] K. Uchida, H. Adachi, T. Kikkawa, A. Kirihara, M. Ishida, S. Yorozu, S. Maekawa, and E. Saitoh, Proc. IEEE **104**, 1946 (2016).

[33] M. Mizuguchi and S. Nakatsuji, Sci. Technol. Adv. Mater. **20**, 262 (2019).

[34] X. Yan, G. Joshi, W. Liu, Y. Lan, H. Wang, S. Lee, J. W. Simonson, S. J. Poon, T. M. Tritt, G. Chen, and Z. F. Ren, Nano Lett. **11**, 556 (2011).

[35] S. R. Boona, K. Vandaele, I. N. Boona, D. W. McComb, and J. P. Heremans, Nat. Commun. **7**, 13714 (2016).

26 May 2024 05:25:59

Applied Physics Letters ACCEPTED MANUSCRIPT
This is the author's peer reviewed, accepted manuscript. However, the online version of record will be different from this version once it has been copyedited and typeset.
PLEASE CITE THIS ARTICLE AS DOI: 10.1063/1.5131001
AIP Publishing

FIG. 1. (a),(b) Schematic illustrations of AEE in a permanent magnet in the in-plane magnetized (a) and perpendicularly magnetized (b) configurations. $\mathbf{J}_c$ and $\mathbf{J}_{q,AEE}$ denote the charge current applied to the magnet and heat current driven by AEE, respectively. In both the configurations, **M** shows the direction of the remanent magnetization, which is along the *c* axis of the magnet. (c),(d) Lock-in amplitude *A* and phase ϕ images for the $SmCo_5$ slab in the in-plane magnetized (c) and perpendicularly magnetized (d) configurations at the charge current magnitude J_c=0.4 A and lock-in frequency *f*=2.0 Hz. The surface *A* and ϕ profiles along the *z* direction are also shown, which are extracted around the center of the thermal images. (e) J_c dependence of *A* for the $SmCo_5$ slab in the in-plane magnetized configuration at *f*=2.0, 5.0, and 25.0 Hz. (f) Steady-state infrared image for the black-ink-coated $SmCo_5$ slab and setup for the LIT measurements. The data points in (e) were obtained by averaging the temperature modulation signals on the area defined by the white rectangle with the size of 51×101 pixels in (f). The results shown in this figure were obtained from the $SmCo_5$ slab with the saturation magnetization of $\mu_0 M_s$=1.01 T.

FIG. 2. *f* dependence of A/j_c for the $SmCo_5$ slab with $\mu_0 M_s$=1.01 T (red squares) and the Ni slab (black circles) in the in-plane magnetized configuration. j_c is the amplitude of the square-wave-modulated charge current density applied to the slabs, which is smaller than the sinusoidal amplitude by a factor of $\pi/4$ (note that the sinusoidal amplitude of the charge current density was used to estimate Π_{AEE} from the LIT data). The LIT measurements for the $SmCo_5$ slab were performed in the absence of the external magnetic field **H**, while the data for the Ni slab were measured with applying **H** with the magnitude $\mu_0 H$=0.6 T in the direction perpendicular to $\mathbf{J}_c$. At 0.6 T, the magnetization of the Ni slab aligns along the **H** direction. The solid red and black lines show the calculated *f* dependence of A/j_c for the $SmCo_5$ and Ni slabs, respectively, which were obtained by solving the one-dimensional heat diffusion equation.

FIG. 3. (a) $\mu_0 M_s$ dependence of the anomalous Ettingshausen coefficient Π_{AEE} and corresponding anomalous Nernst coefficient S_{ANE} ($=\Pi_{AEE}/T$) for the $SmCo_5$-type magnets (red squares), Sm_2Co_{17}-type magnets (blue circles), $Nd_2Fe_{14}B$-type magnet (green triangle), and Ni (black diamond) at temperature *T*=300 K. The data point for the $SmCo_5$-type magnet with $\mu_0 M_s$=1.01 T, used for the experiments in Figs. 1 and 2, is emphasized by changing its color.

26 May 2024 05:25:59

Applied Physics Letters ACCEPTED MANUSCRIPT
This is the author's peer reviewed, accepted manuscript. However, the online version of record will be different from this version once it has been copyedited and typeset.
PLEASE CITE THIS ARTICLE AS DOI: 10.1063/1.5131001

All the AEE measurements shown in this figure were performed in the in-plane magnetized configuration. (b) $\mu_0 M_s$ dependence of the dimension-less figure of merit $Z_{AEE}T$ for AEE in the magnets at T=300 K and the Z_{AEE} values normalized by the value of Ni. The insets to (b) show the $\mu_0 M_s$ dependence of the longitudinal electric conductivity σ_{xx} and the thermal conductivity κ of the magnets. Despite being out of range in the insets, the σ_{xx} and κ values of Ni were observed to be 12.2×10^6 Sm^{-1} and 76.4 $WK^{-1}m^{-1}$, respectively.

FIG. 4. (a) $\mu_0 H$ dependence of the Hall resistivity ρ_{Hall} for the $SmCo_5$-, Sm_2Co_{17}-, and $Nd_2Fe_{14}B$-type magnets. The results shown in this figure were obtained from the $SmCo_5$-type, Sm_2Co_{17}-, and $Nd_2Fe_{14}B$-type magnets with $\mu_0 M_s$=1.01 T, 1.14 T, and 1.50 T, respectively (Table S1 in supplementary material). (b) Anomalous Hall angle θ_{AHE} of the magnets. The inset to (b) shows the σ_{xx} dependence of the transverse electric conductivity σ_{xy} for the $SmCo_5$-type magnet (red square), Sm_2Co_{17}-type magnet (blue circle), and $Nd_2Fe_{14}B$-type magnet (green triangle), where the σ_{xy} values were obtained by extrapolating the ρ_{Hall} data in the high-field region (9 T<$\mu_0 H$<10 T) to the zero field. (c) Seebeck coefficient S_{xx} of the magnets. The S_{xx} values were estimated by measuring the electric voltage V along the temperature gradient ∇T. We confirmed that the magneto-Seebeck effect[8,10] in the magnets is negligibly small by repeating the thermopower measurements after demagnetization. (d) Π_I and Π_{II}, defined by Eq. (3), of the magnets at T=300 K. (e) Transverse thermoelectric conductivity α_{xy} at T=300 K for the $SmCo_5$-, Sm_2Co_{17}-, and $Nd_2Fe_{14}B$-type magnets and the full-Heusler Co_2MnGa. The α_{xy} values of Co_2MnGa for different configurations were estimated from Fig. 3 of Ref. 20, where **M** is parallel to the [111], [110], or [100] direction of Co_2MnGa.

26 May 2024 05:25:59

AIP Publishing

Applied Physics Letters ACCEPTED MANUSCRIPT

This is the author's peer reviewed, accepted manuscript. However, the online version of record will be different from this version once it has been copyedited and typeset.

PLEASE CITE THIS ARTICLE AS DOI: 10.1063/1.5131001

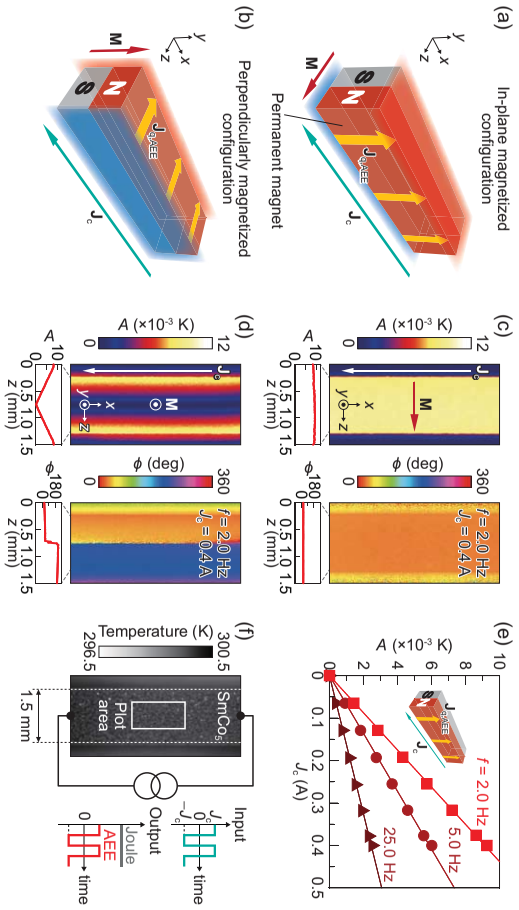

26 May 2024 05:25:59

AIP Publishing

Applied Physics Letters ACCEPTED MANUSCRIPT

This is the author's peer reviewed, accepted manuscript. However, the online version of record will be different from this version once it has been copyedited and typeset.

PLEASE CITE THIS ARTICLE AS DOI: 10.1063/1.5131001

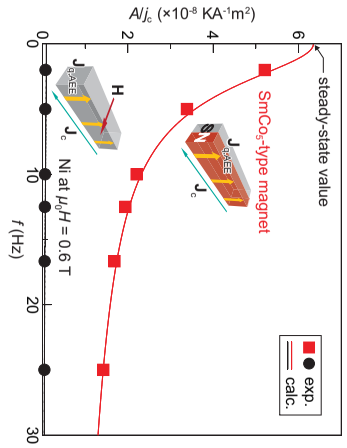

26 May 2024 05:25:59

AIP Publishing

Applied Physics Letters ACCEPTED MANUSCRIPT

This is the author's peer reviewed, accepted manuscript. However, the online version of record will be different from this version once it has been copyedited and typeset.

PLEASE CITE THIS ARTICLE AS DOI: 10.1063/1.5131001

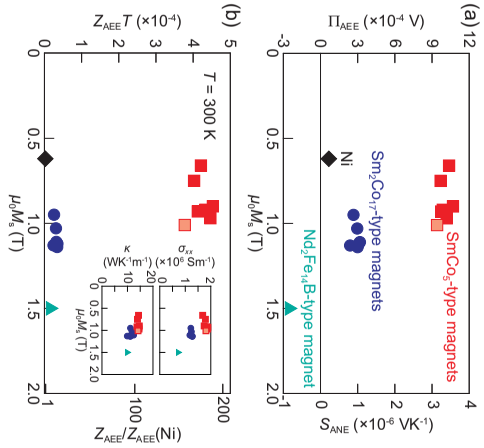

26 May 2024 05:25:59

AIP Publishing

Applied Physics Letters ACCEPTED MANUSCRIPT

This is the author's peer reviewed, accepted manuscript. However, the online version of record will be different from this version once it has been copyedited and typeset.

PLEASE CITE THIS ARTICLE AS DOI: 10.1063/1.5131001

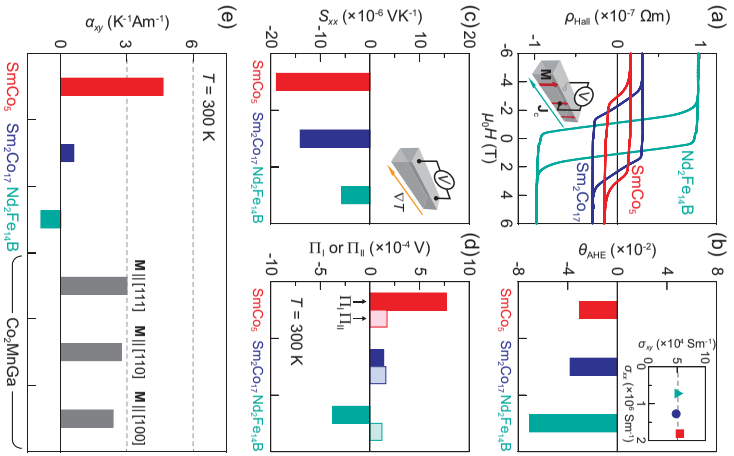

26 May 2024 05:25:59